The last glacial cycle: transient simulations with an AOGCM

The last glacial cycle: transient simulations with an AOGCM

Robin S. Smith & Jonathan Gregory

Climate Dynamics
Observational, Theoretical and Computational Research on the Climate System

ISSN 0930-7575

Clim Dyn
DOI 10.1007/s00382-011-1283-y

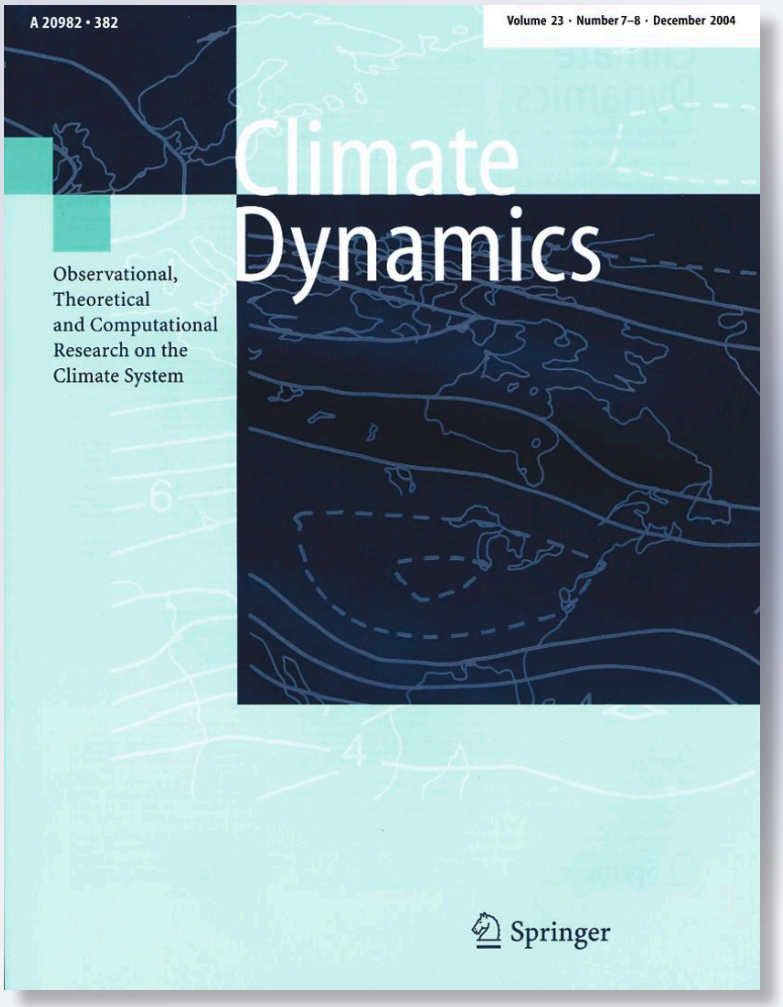

Springer

Clim Dyn
DOI 10.1007/s00382-011-1283-y

The last glacial cycle: transient simulations with an AOGCM

Robin S. Smith · Jonathan Gregory

Received: 10 November 2010 / Accepted: 26 December 2011

Abstract A number of transient climate runs simulating the last 120 kyr have been carried out using FAMOUS, a fast atmosphere–ocean general circulation model (AOGCM). This is the first time such experiments have been done with a full AOGCM, providing a three-dimensional simulation of both atmosphere and ocean over this period. Our simulation thus includes internally generated temporal variability over periods from days to millennia, and physical, detailed representations of important processes such as clouds and precipitation. Although the model is fast, computational restrictions mean that the rate of change of the forcings has been increased by a factor of 10, making each experiment 12 kyr long. Atmospheric greenhouse gases (GHGs), northern hemisphere ice sheets and variations in solar radiation arising from changes in the Earth's orbit are treated as forcing factors, and are applied either separately or combined in different experiments. The long-term temperature changes on Antarctica match well with reconstructions derived from ice-core data, as does variability on timescales longer than 10 kyr. Last Glacial Maximum (LGM) cooling on Greenland is reasonably well simulated, although our simulations, which lack ice-sheet meltwater forcing, do not reproduce the abrupt, millennial scale climate shifts seen in northern hemisphere climate proxies or their slower southern hemisphere counterparts. The spatial pattern of sea surface cooling at the LGM matches proxy reconstructions reasonably well. There is significant anti-correlated variability in the strengths of the Atlantic meridional overturning circulation (AMOC) and the Antarctic Circumpolar Current (ACC) on timescales greater than 10 kyr in our experiments. We find that GHG forcing weakens the AMOC and strengthens the ACC, whilst the presence of northern hemisphere ice-sheets strengthens the AMOC and weakens the ACC. The structure of the AMOC at the LGM is found to be sensitive to the details of the ice-sheet reconstruction used. The precessional component of the orbital forcing induces ~20 kyr oscillations in the AMOC and ACC, whose amplitude is mediated by changes in the eccentricity of the Earth's orbit. These forcing influences combine, to first order, in a linear fashion to produce the mean climate and ocean variability seen in the run with all forcings.

R. S. Smith (✉) · J. Gregory
NCAS-Climate, Department of Meteorology,
University of Reading, Reading, UK
e-mail: r.s.smith@reading.ac.uk

J. Gregory
Met Office Hadley Centre, Exeter, UK

1 Introduction

The glacial cycles of the last million years are the largest climatic variations to have occurred within the period of human evolution (Jouzel et al. 2007; Lisiecki and Raymo 2005), yet despite the existence of climate proxy data for the last glacial cycle that provide almost global coverage at a variety of temporal resolutions, from seasonal to millennial, there are still large gaps in our knowledge of how the climate evolves through a glacial cycle.

It is generally accepted that the timing of glacials is linked to variations in solar insolation that result from the Earth's orbit around the sun (Hays et al. 1976; Huybers and Wunsch 2005). These solar radiative anomalies must have been amplified by feedback processes within the climate system, including changes in atmospheric greenhouse gas (GHG) concentrations (Archer et al. 2000) and ice-sheet growth (Clark et al. 1999), and whilst hypotheses abound as to the details of these feedbacks, none is without its

Published online: 12 January 2012

detractors and we cannot yet claim to know how the Earth system produced the climate we see recorded in numerous proxy records. This is of more than purely intellectual interest: a full understanding of the carbon cycle during a glacial cycle, or the details of how regional sea-level changed as the ice-sheets waxed and waned would be of great use in accurately predicting the future climatic effects of anthropogenic CO_2 emissions, as we might expect many of the same fundamental feedbacks to be at play in both scenarios.

Analysis of climate proxies found in ocean sediments, ice-cores and other sources yields a wealth of information, but detailed climate reconstructions from such data are limited by the significant uncertainties that arise from the multiple signals that are recorded in each proxy, uncertainty in accurately dating them, and their spatial representativeness (e.g. Wolff et al. 2010). Computer models of the climate system are thus invaluable tools that can help to interpret the proxies, fill in gaps where we have no data and test different hypotheses of the evolution of the climate.

The multi-millennial timescales involved in modelling even a single glacial cycle present an enormous challenge to comprehensive Earth system models based on coupled atmosphere–ocean general circulation models (AOGCMs). Due to the computational expense involved, AOGCMs are usually limited to runs of a few hundred years at most, and their use in paleoclimate studies has generally been through short, "snapshot" runs of specific periods of interest (e.g. Braconnot et al. 2007; Lunt et al. 2008). Transient simulations of glacial cycles have hitherto only been run with models where important climate processes such as clouds or atmospheric moisture transports are more crudely parameterised than in an AOGCM or omitted entirely (e.g. Marsh et al. 2006; Ganopolski et al. 2010; Holden et al. 2010). The heavy restrictions on the feedbacks involved in such models limit what we can learn of the evolution of the climate from them, particularly in paleoclimate states that may be significantly different from the better-known modern climates which the models are formulated to reproduce. Simulating past climate states in AOGCMs and comparing the results to climate reconstructions based on proxies also allows us to test the models' sensitivities to climate forcings and build confidence in their predictions of future climate.

Here we present the first AOGCM transient simulations of the whole of the last glacial cycle. We have reduced the computational expense of these simulations by using FAMOUS, an AOGCM with a relatively low spatial resolution, and by accelerating the boundary conditions that we apply by a factor of ten, such that the 120,000 year cycle occurs in 12,000 years. We investigate how the influences of orbital variations in solar irradiance, GHGs and northern hemisphere ice-sheets combine to affect the evolution of the climate, comparing our simulations with both proxy-based climate reconstructions and previous model studies. We also investigate how the large-scale ocean circulation changes during the simulations. A comprehensive analysis of all aspects of the climate system of these runs is beyond the scope of any one paper, and we shall restrict this study to a few large-scale features in the interests of brevity.

The paper is arranged as follows. We outline the model that we use in Sect. 2, and describe the experimental setup in Sect. 3. Section 4 introduces our results by way of comparisons with proxy-based climate reconstructions and other models, and Sect. 5 looks at how the global-average glacial climate relates to that at polar latitudes. Section 6 investigates the transient response of the ocean circulation and its influence on the climate, following which we conclude in Sect. 7 with a discussion of our results.

2 Model

For these simulations we use FAMOUS (FAst Met. Office and UK universities Simulator) (Jones et al. 2005; Smith et al. 2008) a low resolution version of the Hadley Centre Coupled Model (HadCM3) AOGCM (Gordon et al. 2000). FAMOUS has approximately half the spatial resolution of HadCM3, which reduces the computational cost of the model by a factor of 10. The ocean component is based on the rigid-lid Cox-Bryan model (Pacanowski et al. 1990), and is run at a resolution of 2.5° latitude by 3.75° longitude, with 20 vertical levels. The atmosphere is based on the primitive equations, with a resolution of 5° latitude by 7.5° longitude with 11 vertical levels (see Table 1).

Version XDBUA of FAMOUS (simply FAMOUS hereafter, see Smith et al. (2008) for full details) has a preindustrial control climate that is reasonably similar to that of HadCM3, although FAMOUS has a high latitude cold bias in the northern hemisphere during winter of about 5°C with respect to HadCM3 (averaged north of 40°N), and a consequent overestimate of winter sea-ice extent in the

Table 1 Table comparing the resolutions of FAMOUS and HadCM3

	Model	
	HadCM3	FAMOUS
Atmosphere resolution (latitude × longitude), (vertical levels)	2.50° × 3.75°, 19	5.00° × 7.50°, 11
Atmosphere timestep (mins)	30	60
Ocean resolution (latitude × longitude), (vertical levels)	1.25° × 1.25°, 20	2.5° × 3.75°, 20
Ocean timestep (mins)	60	720

North Atlantic. The global climate sensitivity of FAMOUS to increases in atmospheric CO_2 is, however, similar to that of HadCM3. FAMOUS incorporates a number of differences from HadCM3 intended to improve its climate simulation—for example, Iceland has been removed (Jones 2003) to encourage more northward ocean heat transport in the Atlantic. Smith and Gregory (2009) demonstrate that the sensitivity of the Atlantic meridional overturning circulation (AMOC) to perturbations in this version of FAMOUS is in the middle of the range when compared to many other coupled climate models.

The model used in this study differs from XDBUA FAMOUS in that two technical bugs in the code have been fixed. Latent and sensible heat fluxes from the ocean were mistakenly interchanged in part of the coupling routine, and snow falling on sea-ice at coastal points was lost from the model. Correction of these errors results in an additional surface cold bias of a degree or so around high latitude coastal areas with respect to XDBUA, but no major changes to the model climatology. In addition, the basic land topography used in these runs was interpolated from the modern values in the ICE-5G dataset (Peltier 2004), which differs somewhat from the US Navy-derived topography used in Smith et al. (2008) and HadCM3.

3 Experiments

The aim of this study is to investigate the physical climate of the atmosphere and ocean through the last glacial cycle. Along with changes in solar insolation that result from variations in the Earth's orbit around the sun, we treat northern hemisphere ice-sheets and changes in the GHG composition of the atmosphere as external forcing factors of the climate system which we specify as boundary conditions, either alone or in combination. Changes in solar activity, Antarctic ice, surface vegetation, or sea-level and meltwater fluxes implied by the evolving ice-sheets are not included in these simulations. Our experimental setup is thus somewhat simplified, with certain potential climate feedbacks excluded. Although partly a matter of necessity due to missing or poorly modelled processes in this version of FAMOUS, this simplification allows us to more clearly see the influence of the specified forcings, as well as ensuring that the simulations stay close to the real climate.

Despite the computational cost of FAMOUS being an order of magnitude lower than most AOGCMs, a 120,000 year climate simulation is still an impractical proposition. Therefore, each of the external forcings has been accelerated by a factor of ten, such that each experiment sees 120,000 years of forcing variation applied over a 12,000 year period. The adjustment timescales of atmospheric and surface climate processes are fast enough that the acceleration of the external forcings will have little effect on them, and there is support in the literature for the accuracy of this approximation when considering the surface climate (Timm and Timmermann 2007; Ganopolski et al. 2010). Adjustment timescales in the deep ocean, however, are on the order of thousands of years, and the acceleration of the external forcings will have an impact there, as will be discussed later. In the rest of this paper, dates and timescales in the model simulations will all be mapped onto a non-accelerated time-axis (i.e. multiplied by a factor of ten) to aid comparison with events and processes recorded in proxy datasets.

Five experiments will be used for the majority of the analysis in this paper (Table 2). All the experiments start from a climate state intended to be analogous to the last interglacial, with orbital insolation parameters appropriate for 120 kyr BP and preindustrial topography, ice-sheets and GHG concentrations.

There are three experiments which assess the influence of the climate forcing factors separately. ORB is forced just with changes in the latitudinal distribution of solar irradiance (Berger 1978). GHG is forced with spatially-constant atmospheric concentrations of CO_2, CH_4 and N_2O, as reconstructed in the EPICA Project (Lüthi et al. 2008; Spahni et al. 2005) mapped onto the EDC3 (Parrenin et al. 2007 age scale). Experiment ICE is forced with surface elevations and ice-sheet extent data taken from the modelling study of Zweck and Huybrechts (2005) which was forced with climate data from a different version of the UKMO model (Hewitt and Mitchell 1997). Due to the limited spatial extent of the ice-sheet model and to facilitate comparison with the other runs, ice-sheet forcing (including isostatic effects on non-ice-sheet topography) is only applied north of 40°N.

Two further experiments combine the three climate forcing factors considered in our study. ALL-ZH applies all the forcings described above together. ALL-5G differs from ALL-ZH in that the topographic and ice-sheet forcings are derived from the ICE-5G v1.2 dataset (Peltier 2004). Topographic changes in this run are also restricted to the region north of 40°N. Before the Last Glacial Maximum (LGM), a lack of data means it is difficult to reconstruct the extent of the ice-sheets; testing two

Table 2 Table of the principal experiments

Experiment	Orbital	GHG	Ice-sheet
ORB	Transient	120 kyr	Preindustrial
GHG	120 kyr	Transient	Preindustrial
ICE	120 kyr	120 kyr	Zweck and Huybrechts (2005)
ALL-ZH	Transient	Transient	Zweck and Huybrechts (2005)
ALL-5G	Transient	Transient	Peltier (2004)

different reconstructions allows us to assess the impact of this uncertainty. It should be noted that the ICE-5G ice-sheets from 120 kyr up to the LGM are fixed at their LGM extent for the whole period, varying only in height, with the total volume constrained by the SPECMAP record Martinson et al. (1987). Ice extent is thus overestimated for much of the ALL-5G simulation. This ice-sheet reconstruction was also used by Singarayer and Valdes (2010) (SV10 hereafter), who conducted a series of snapshot runs over the last glacial cycle with HadCM3, FAMOUS's parent model, and we will compare the results from ALL-5G with those of SV10. To avoid confusion when comparing runs with different ice-sheet reconstructions, in this paper we define the LGM as occurring at 22 kyr BP, when atmospheric CO_2 levels were at their lowest (Lüthi et al. 2008).

Our configuration of FAMOUS only allows ice-sheets to be specified where there is land; as sea-level does not change in these experiments, the interpolated ice-sheets are not allowed to extend over modern ocean points. This issue affects our use of both the Zweck and Huybrechts (2005) and ICE-5G reconstructions, particularly with respect to the Fennoscandian ice-sheet. However, once interpolated onto the FAMOUS grid (which is coastally-tiled, so allows for gridboxes to have both land and ocean properties on the atmosphere grid), both reconstructions are approximately equally affected, and this restriction on the ice-sheet area does not unduly influence the comparison of the effects of the different ice-sheet reconstructions.

4 Comparisons with climate proxies

The proxies from which past climate is reconstructed are not equivalent to direct observations of a given climate variable. Reconstructing climate from proxy measurements implicitly requires some kind of model, and the proxies are, in general, influenced by combinations of different factors. Wolff et al. (2010) reviews the interpretation of ice-core data. This makes comparison of climate model output with the proxy data non-trivial. The most straightforward comparison with the measured data would be to include models of the proxies within the climate model, but such models are not present in this version of FAMOUS (although the oxygen isotope scheme of Tindall et al. (2009) has now been implemented for future use).

In this section, we compare the output from our ALL-ZH and ALL-5G runs with surface temperature reconstructions from three different proxy datasets. Throughout we will rely on the conversions and corrections applied to the data by the authors of those reconstructions. In addition, we refer to results from SV10, who conducted a series of snapshot simulations covering the last glacial cycle with HadCM3, and the Paleo-Modelling Intercomparison Project phase 2 (PMIP2, Braconnot et al. 2007), which set out common boundary conditions and conducted an intercomparison of LGM climates from a number of different models. Our comparisons will be largely descriptive, with further discussion of notable features to be found in the next section.

4.1 Antarctica

The EPICA ice-core from Dome C, Antarctica (75°S, 123°E) is one of the longest, most detailed records of Quaternary climate, covering the last 8 glacial cycles. For comparison with the EPICA temperature reconstruction of Jouzel et al. (2007), we take modelled surface temperatures from the corresponding gridbox in our model (taking a local area average makes no significant difference). The proxy reconstruction is corrected for changes in surface elevation, so the comparison with our simulations, where the height of the Antarctic ice-sheet does not change, is valid. The reconstruction is not adjusted for changes in the seasonality of precipitation as these are believed to be small at Dome C. We have not weighted our simulations by precipitation: the seasonal cycle of precipitation on Antarctica does change in our simulations, but given the complexity of modelling Antarctic precipitation and the low resolution of our model, we do not view our simulated changes as robust.

A broad comparison of both ALL-ZH and ALL-5G with the EPICA curve shows that the climate sensitivity of the model is about right (Fig. 1, above). There is a maximum temperature anomaly of around −10°C in both runs, comparable to the LGM temperature anomaly in the EPICA reconstruction. The timing of the maximum cooling in our simulations occurs about 5 kyr earlier than in the reconstruction, correlating with a minimum in the local orbital forcing. Masson-Delmotte et al. (2010) note that, whilst the PMIP2 models find temperature changes of a similar magnitude in this region, about half of the PMIP2 change can be ascribed to the change in ice-sheet altitude specified in the PMIP2 protocol whose influence has already been allowed for and removed from the EPICA record. They thus infer that the PMIP2 models, unlike FAMOUS, largely underestimated the magnitude of Antarctic cooling at the LGM. The overall rate of cooling during the glaciation, at ~ -0.1 K/kyr, matches the EPICA record well, but both ALL-ZH and ALL-5G cool too slowly at inception, around 120 kyr BP. The EPICA data shows that, relative to their respective longer term trends, temperature fell more rapidly than CO_2 during this period, but in our experiments simulated Antarctic temperatures drop in line with CO_2. This suggests that there is an important missing feedback in our model, or that our model

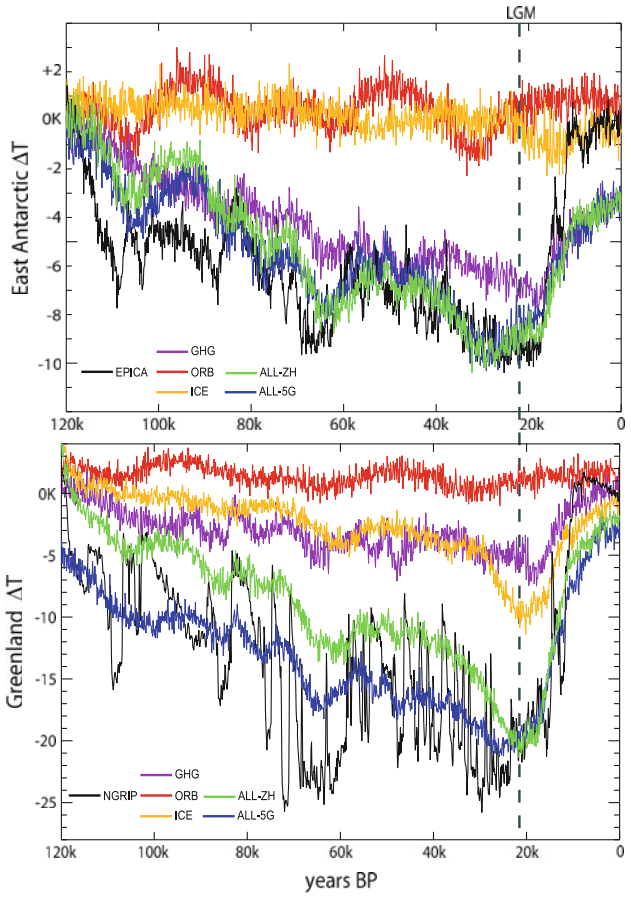

Fig. 1 East Antarctic (*above*) and Greenland (*below*) surface temperature differences from preindustrial

is perhaps over-sensitive to CO_2, and under-sensitive to one of the other forcing factors. Tests of the model where the forcings were not artificially accelerated rule out the possibility of the acceleration being a factor. The only forcing that is rapidly changing during this time is the seasonality of the orbital forcing, but as the amplitude of the multi-millennial (>10 kyr) oscillations in between 100 kyr and 20 kyr BP (Fig. 1, above) are approximately correct, this is not a likely explanation. Holden et al. (2010) suggest that the absence of a West Antarctic ice-sheet is necessary to explain the reconstructed high temperatures of the last interglacial; the regrowth of the West Antarctic ice-sheet may help explain the discrepancy here in the rate of temperature change at inception.

After the LGM, and especially after ~10 kyr, Antarctic temperatures in our simulation rise much more slowly than in reality. This is a result of the accelerated nature of our simulations. Cold deep ocean water is returned to the surface of the Southern Ocean in our simulations during this period, and as our deep Southern Ocean takes around 500 years to begin responding to the change in surface conditions, this water does not have enough time to warm sufficiently in these accelerated model runs. The impact of the acceleration of the forcing on the ocean circulation is discussed later. This cold upwelling anomaly is only found at high southern latitudes in our simulations. Surface temperatures for the rest of the world (with the exception of Greenland, discussed later) at the end of the ALL experiments are within 0.5 K of our preindustrial simulation, so this cold anomaly noted here does not represent a global problem with our experimental setup.

Variability with significant peaks at frequencies of ~20 and ~40 kyr is superimposed on the long-term cooling trend during glaciation in our simulations. This matches with the precessional and obliquity components of variability in the orbital forcing which modulate the strength of the seasonal cycle. Variability at millennial frequencies identified in the EPICA record, such as the warm events of so-called Antarctic Isotopic Maxima events (EPICA Community Members 2006) or the warming/cooling signal of the Bolling-Allerod/Younger Dryas period do not appear to be present in our simulations.

SV10's multiple snapshot results for Antarctica are qualitatively similar to ALL-5G in many ways, although the amplitude of the orbitally-forced variability in their runs is much less than in ours, providing a poorer match to the EPICA reconstruction, and they also underestimate the maximum cooling at the LGM. As with the PMIP2 runs, SV10 specified an increase in the height of the Antarctic ice-sheet, a factor that has already been removed from the EPICA temperature reconstruction. The inclusion of idealised northern hemisphere meltwater events in some of SV10's simulations does not appear to induce significant Antarctic warm events, but the snapshot nature of their experimental setup not best suited for the simulation of such transient events.

4.2 Greenland

Continuous, high frequency records of climate have also been retrieved from Greenland ice-cores in the northern hemisphere, although the fact that the local climate and ice-sheet topography is more variable than that on Antarctica makes the untangling of a temperature signal from the different influences on the ice much harder. The recent NGRIP core from central Greenland (75°N, 42°W) covers the whole of the last glacial cycle, and the surface temperature reconstruction of Masson-Delmotte et al. (2005) corrects for changes in the isotopic composition of the source water forming the ice, as well as significant biases thought to be attributable to changes in the seasonality of Greenland precipitation. Changes in the elevation of the Greenland ice-sheet are not corrected for; as such, a direct comparison with surface temperature from our simulations is valid, as the Greenland topography we specify is also time-dependent.

Greenland temperatures (averaged between 70–80°N and 35–50°W) in our simulations generally underestimate the changes derived from the ice-core, suggesting that the model's climate sensitivity for this specific region is too low (Fig. 1, below). The maximum temperature anomaly derived from the ice-core is almost -30°C, whilst it is around -20°C in both ALL-ZH and ALL-5G. Previous studies, however, have underestimated LGM temperatures on Greenland by larger amounts, with Hewitt et al. (2003), who used FAMOUS's higher resolution parent model HadCM3 finding a change of ~ -15°C, and -10 to >-15°C being the multi-model average of the PMIP2 study. In this context our results are encouraging.

As with Antarctic temperatures, the model cannot reproduce the rapid rate of cooling at glacial inception, except in ALL-5G where there is the sudden introduction of very thin, LGM-extent ice-sheets on North America and Scandinavia and a large consequent change in surface albedo. Since this forcing is rather unphysical, the model cannot be said to have correctly reproduced the real climate. The surface temperature change on Greenland during the deglaciation does not show a Bolling-Allerod/Younger Dryas period, and retains a cold bias with respect to the preindustrial model state at the end of the experiment. This cold bias is local to Greenland, and is due to a small difference in the heights of the ice-sheets that exist at the end of the experiments and as used in the preindustrial run.

The other striking difference between the model and the NGRIP reconstruction is the model's lack of the abrupt, millennial scale events of large amplitude in the ice-core data. It is thought that periodic surges of meltwater from the northern hemisphere ice-sheets and subsequent disruption of oceanic heat transports are involved in these events (Bond et al. 1993; Blunier et al. 1998), and the lack of ice-sheet meltwater runoff in our model is probably a large part of the reason why we do not simulate them. However, the dust record from Greenland ice-cores has been interpreted by some authors as showing that changes in the atmospheric circulation over Greenland precede the temperature changes (Thomas et al. 2009), implying that ocean heat transport changes may be a consequence, not a trigger, of these abrupt events. Dust is not explicitly modelled in our simulations, but no abrupt shifts in the large-scale atmospheric circulation over Greenland occur in our runs, implying that if a non-oceanic trigger does exist for these abrupt events, we have not reproduced it. Wunsch (2006) has further suggested that these features in Greenland ice-cores may be simply indicative of local changes in the atmospheric circulation at high latitudes as the wind interacts with the growing ice-sheets, and do not robustly reflect widespread climatic events at all. We find no evidence in support of this hypothesis either, although it may be that the model's resolution, which restricts both the representation of ice-sheet topography and atmospheric variability, is a limiting factor. Taken together, the lack of both millennial scale warm events in the south and abrupt events in the north strongly imply a missing feedback of some importance in our model.

As for Antarctica, SV10's simulation of Greenland temperatures is qualitatively similar to ours, although smaller in overall amplitude. They too match the rapid pace of cooling at glacial inception when including the unphysical early ICE-5G extent forcing, but simulate less cooling at the LGM than in our simulations, achieving approximately half of the LGM cooling inferred from the NGRIP ice-core. SV10's simulation without ice-sheet forcing suggests that a significant difference between FAMOUS and HadCM3 here lies in the sensitivity of Greenland temperatures to GHG forcing. Previous studies have shown that FAMOUS and HadCM3 have very similar global climate sensitivities to increased CO_2 concentrations (Smith et al. 2008), but comparing SV10's results with our GHG run suggests that FAMOUS's sensitivity to reduced CO_2 at high latitudes is somewhat greater than HadCM3. SV10's idealised meltwater event simulations do produce significant extra cooling on Greenland, although not enough to fully reconcile their results with the NGRIP reconstruction despite using a very large meltwater forcing.

4.3 LGM surface temperatures

The ice-core-based temperature reconstructions discussed above cover the whole of the time period simulated in our runs, but give little spatial information about the climate. The MARGO project has synthesised 696 SST proxy records to produce an estimate of the spatial pattern of sea surface temperature anomalies at the LGM (defined here as between 23 and 19 kyr BP) (MARGO Project Members 2009). There are also a number of higher-resolution modelling studies that consider just the LGM that we may compare against (Hewitt et al. 2003; Braconnot et al. 2007).

The LGM climates from ALL-ZH and ALL-5G broadly match those of the PMIP2 ensemble, despite differences in the specification of LGM boundary conditions between our runs and PMIP2. The global mean surface air temperature cooling at the LGM in ALL-ZH (4.3°C) (Fig. 2, above) is within the PMIP2 ensemble range of 3.6–5.7°C, as is the maximum temperature anomaly over the Laurentide ice-sheet, at -32°C in ALL-ZH. The greater cooling seen in ALL-5G is due to the greater volume of the ICE-5G ice-sheets in the northern hemisphere.

In agreement with the MARGO data, the maximum SST cooling in ALL-ZH is around 10°C, located in the mid-Atlantic, at about 40°N (Fig. 3). The significant additional cooling provided by the unphysical ALL-5G ice-sheet

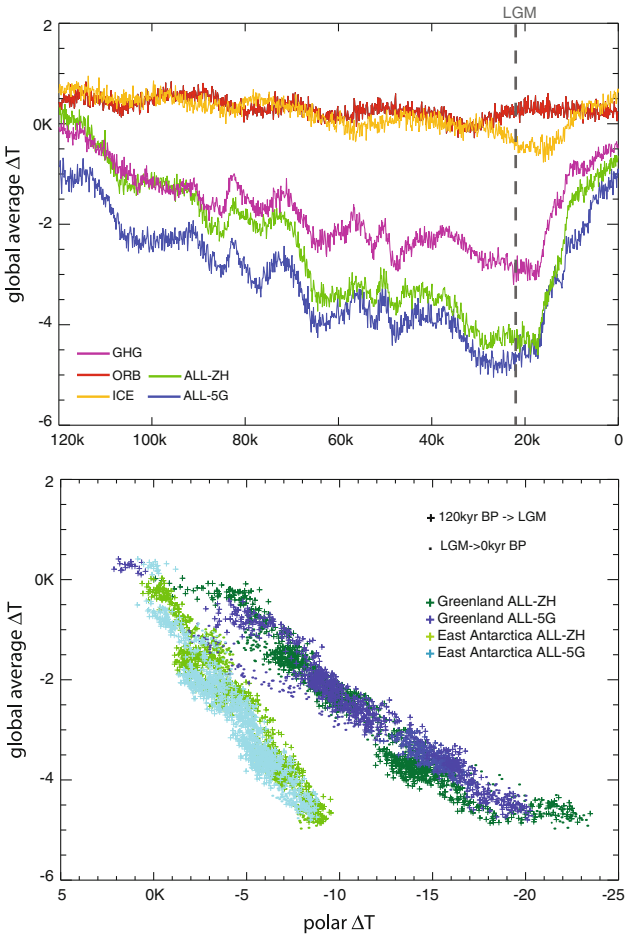

Fig. 2 *Above*: global average surface air temperature anomalies from preindustrial. *Below*: Greenland (*dark colours*) and east Antarctic (*light colours*) anomalies plotted against global average temperature anomalies for the ALL-ZH (*green*) and ALL-5G (*blue*) simulations, showing the polar amplification of the global climate change

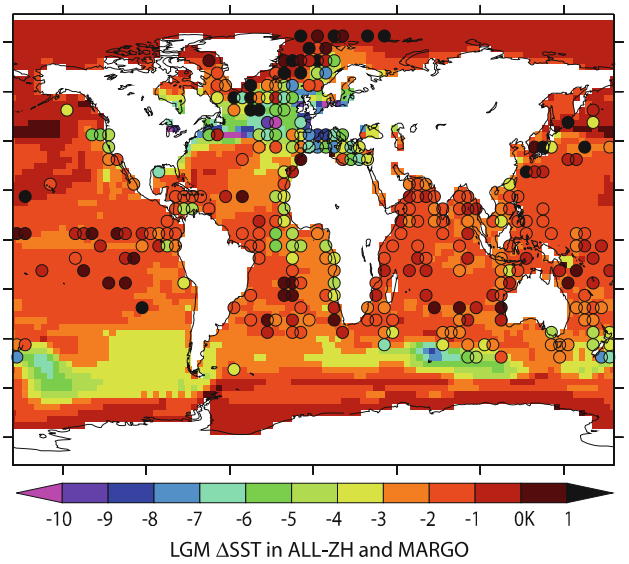

Fig. 3 LGM SST difference from the preindustrial state in the ALL-ZH simulation. *Circles* show the multi-proxy SST anomaly reconstruction of MARGO Project Members (2009)

throughout most of the glacial does little to distinguish the resultant LGM SSTs from the ALL-ZH simulation by the LGM, suggesting that the history of the ice-sheet forcing in may not be too important in this respect in snapshot simulations of LGM climate.

For the tropical area of 30°S:30°N, we find mean a mean SST cooling of −1.8°C in ALL-ZH at the LGM, within the PMIP2 spread of 1.0–2.4°C and in good agreement with the MARGO estimate of 1.7 ± 1.0°C. In common with the PMIP2 models, we do not reproduce the magnitude of the cooling on the eastern side of the Atlantic inferred from the MARGO data. Otto-Bliesner et al. (2009) attribute this failing of the PMIP2 models to common model biases in reproducing the correct geographical variation of thermocline depths and the correct vertical temperature stratification of ocean waters. FAMOUS also suffers from these biases, so its failure to accurately reproduce the cross-basin gradients is not surprising. Also in line with the PMIP2 models, although FAMOUS matches MARGO in producing more LGM cooling in the Atlantic than the Pacific, the magnitude of this inter-basin contrast in FAMOUS is too weak when compared to the MARGO reconstruction.

The subtropical gyre in the North Pacific sees little or no cooling in the ALL experiments. There is some support in the MARGO data for little cooling, or even warming, in this region. In FAMOUS this SST feature is due to a persistent low pressure anomaly over the north Pacific which affects the large-scale atmospheric circulation. This feature is particularly marked in the ICE experiment, where the surface temperature anomaly pattern associated with the full LGM ice-sheet forcing has strong cooling in the Atlantic and a warm anomaly in the Pacific extending down the eastern side of the basin (Fig. 4). This pattern is linked to the presence of a persistent low pressure anomaly in the North Pacific, which induces cyclonic flow in the surface winds that brings warm air up the east side of the Pacific from low latitudes. There is a corresponding cold anomaly on the western side of the Pacific and over north-east Asia. This Atlantic/Pacific temperature dipole was also identified by Justino et al. (2006) as a feature of the climate response to ice-sheet forcing in their model.

5 Relating the high latitudes to global climate

Due to the incomplete spatial coverage of continuous climate proxies through the Pleistocene, the climate reconstructions from the Greenland and Antarctic ice-cores are sometimes used to estimate global climate changes over this period. Projections of both future climate change and reconstructions of past climate show a polar amplification

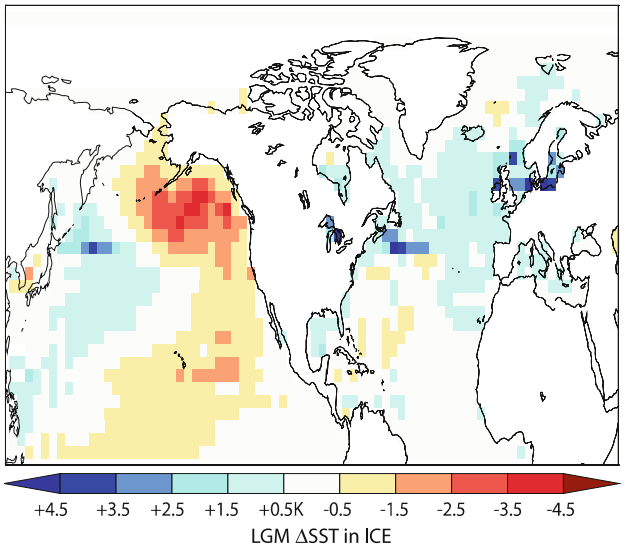

Fig. 4 SST anomaly between maximum and minimum ice-sheet volume states in the ICE run

effect, whereby climate feedbacks act to increase surface temperature changes at high latitudes compared to the tropics (Manabe and Wetherald 1975). To correctly relate ice-core data to the rest of the globe, it is thus important to understand the climate processes involved in polar amplification in the glacial climate system. In this section, we investigate the mechanisms that lead to polar amplification in a colder world, and how they vary through a glacial cycle.

It can be seen from Fig. 1 (below) that the northern hemisphere ice-sheets have a relatively small effect on surface temperatures on East Antarctica in FAMOUS. Temperature variation at Dome C in our experiments is largely explained by the long-term GHG trend, overlaid with ~20 kyr variability contributed by the orbital forcing. The greater Antarctic cooling at the LGM that is seen in the ALL experiments than in the PMIP2 models (once they have been corrected for elevation changes) can thus be attributed to the response to the GHG forcing in FAMOUS. Southern hemisphere sea-ice extent in FAMOUS at the LGM increases more than in the HadCM3 LGM snapshot experiment of Hewitt et al. (2003), and it is likely that this is key to explaining the relatively large Antarctic temperature change in FAMOUS.

Greenland temperatures are also cooler at the LGM than in Hewitt et al. (2003) and the PMIP2 models, although not as cool as reconstructed from NGRIP data. GHG forcing is roughly as important as the ice-sheet forcing in setting this temperature change in FAMOUS (Fig. 1, below). The latter contribution is in part simply due to the ice-sheet reconstruction: ICE-5G has higher LGM ice-sheets than the previous ICE-4G reconstruction used in Hewitt et al. (2003), and Zweck and Huybrechts's (2005) model produces even higher elevations for Greenland.

Poleward heat transport in the LGM climate in FAMOUS is less than in other models too. Justino et al. (2006) analyse the climate response to the ICE-5G reconstruction and identify enhanced surface heat transport in the ocean resulting from increased wind speeds in the mid-Atlantic as an important factor in setting high latitude Atlantic surface temperatures. This process also appears to be at work in Hewitt et al. (2003). Neither ALL-ZH nor ALL-5G simulate large increases in mid-Atlantic surface winds or their associated heat transport for the LGM climate. Amplifying this cooling, as in the southern hemisphere, FAMOUS forms more sea-ice in the northern hemisphere at the LGM than other models. This provides a cooling from the surface albedo forcing, whilst restricting evaporation and contributing further to a drier, colder atmosphere.

The degree of polar amplification (defined as $\left[\frac{\Delta T_{\text{Greenland}}}{\Delta T_{\text{global average}}}\right]$ for the northern hemisphere, and $\left[\frac{\Delta T_{\text{Dome C}}}{\Delta T_{\text{global average}}}\right]$ for the southern) through the glacial cycle is not constant in time. In Fig. 2 (below), we plot global average temperature anomalies from our simulations against the polar anomalies; the slope of the data shows the amount of polar amplification, and the scatter of the data indicates how constant the relationship is. In general there is a strong linear relationship (Table 3) between global average temperatures and those recorded at polar latitudes. It can be seen by eye that Greenland sees a larger amplification of the global average signal than East Antarctica, with a larger degree of scatter in the data. Greenland temperatures in particular decouple from a constant linear amplification of the global temperature anomaly at the LGM (and, to a lesser extent, at the beginning and end of the simulation) when the rate of change of the global anomaly is smallest. This is likely due to the strong local influence of changes in the northern hemisphere ice-sheets. Greenland temperatures also show a slightly different degree of polar amplification during deglaciation than earlier in the run (the slope of the dark dots in Fig. 2 (below) is steeper than for the crosses), suggesting that Antarctic ice-core records are thus likely to make more reliable estimates of global temperature change through glacial cycles.

SV10 also considered the polar amplification found in their multi-snapshot simulation. They found a magnitude

Table 3 Statistics of linear fits to the polar amplification relationship between global average and polar temperature anomalies

Experiment	Slope	Correlation	1-Sigma uncertainty
Greenland ALL-ZH	3.60	0.96	0.032
Greenland ALL-5G	4.10	0.97	0.030
E. Ant. ALL-ZH	1.83	0.97	0.014
E. Ant. ALL-5G	1.74	0.94	0.018

and variability of Antarctic amplification behaviour that was very similar to our FAMOUS results, and we support their conclusion that Antarctic ice-core records are more likely to provide reliable estimates of global temperature changes. Results for Greenland differ more between our results and SV10. FAMOUS shows a higher Greenland amplification factor; this results from the greater temperature change we find over Greenland, as noted in the previous section. Outside of the extreme periods of inception and deglaciation, variability in the Greenland amplification factor also differs between the two models, reinforcing the idea that Greenland temperatures are less reliable indicators of the global mean.

Projections of future climate change forced by CO_2 increase show a stronger polar amplification in the northern hemisphere than in the south. Gregory and Huybrechts (2006) give multi-model averages of 1.1 ± 0.2 for the southern hemisphere, and 1.5 ± 0.4 for the northern hemisphere, and this hemispheric asymmetry is also seen here in the ALL experiments. However, a pure CO_2 forcing is basically hemispherically symmetric, whereas the growth of the northern hemisphere ice-sheets makes the total glacial climate forcing strongly hemispherically asymmetric. Our glacial GHG experiment, which has no ice-sheet influence, has very similar northern and southern polar amplification factors of around 2 (not shown), implying that the climate feedbacks which lead to polar amplification as the climate warms in response to CO_2 do not apply in the same way as the climate cools. The response of sea-ice, in particular, differs between the warming and cooling cases.

To illustrate this we conduct a 400 year idealised CO_2 increase experiment in FAMOUS, where concentrations of atmospheric CO_2 are instantaneously raised to four times their preindustrial value. The climate feedback parameter for FAMOUS under this forcing is 1.10 ± 0.09 W/m^2/K, which is similar to the value found for HadCM3 [1.32 ± 0.08 (Jones et al. 2005)]. In this experiment, the sea-ice extent in the Southern Ocean is reduced by 5.4×10^{12} m^2, $\sim 40\%$ of the total, but there is a loss of 12.5×10^{12} m^2 ($\sim 80\%$) in the North Atlantic and Arctic, giving rise to a hemispherically asymmetric forcing from the resultant surface albedo change. This asymmetry is probably due to the different latitudinal profile of the sea-ice distribution in each hemisphere, and the constant presence of the large Antarctic land ice-sheet in the south. In our glacial GHG experiment, however, both hemispheres gain a similar area of ice as the climate cools: 6.8×10^{12} m^2 ($\sim 49\%$) in the Southern Ocean, and 6.3×10^{12} m^2 ($\sim 40\%$) in the North Atlantic and Arctic. The surface albedo feedback is thus hemispherically symmetric for GHG cooling, but asymmetric for CO_2 warming.

6 Ocean circulation dynamics

Variations in the strength of the AMOC and its associated heat transport are thought to be capable of significantly influencing large-scale climate patterns (e.g. Vellinga and Wood 2002), and are widely theorised to be explicitly involved in the large, abrupt changes seen in proxy records of northern hemisphere temperatures over the last glacial cycle (e.g. Bond et al. 1993). The restricted spatial coverage of proxies for ocean circulation means that it is impossible to accurately reconstruct this aspect of the climate system purely from proxy data. Wind and surface buoyancy input are crucial forcings for the large-scale ocean circulation, so the use of a model which explicitly simulates the atmospheric circulation (i.e. a GCM) is important. Previous studies have shown that the sensitivity of FAMOUS to forced changes in the AMOC is in good agreement with other coupled models (Smith and Gregory 2009), which lends some confidence to our interpretation of the ocean circulation changes we simulate. Without glacial meltwater forcing in our simulation, we are not going to reproduce the full ocean circulation through a glacial cycle; we can, however, show how the forcing factors we do include influence the ocean and how those influences combine, to build up a process-based understanding of how the glacial ocean circulation might operate.

The acceleration of the external forcings applied to our simulations might be expected to present more of a problem here, as the timescales of the accelerated orbital forcing (around 2,000 years for precession) overlap with the adjustment timescales of the deep ocean. Experience with FAMOUS shows that the AMOC and Antarctic Circumpolar Current (ACC) spin up to perturbed boundary conditions over periods of around 500 years, similar to the time lag between the change in surface forcing and the initial response of the deep Southern Ocean after the LGM in our GHG experiment (not shown). Whilst the ocean circulation response to the accelerated forcings may thus be somewhat distorted, it is unlikely to be qualitatively incorrect, at least in the period between the last interglacial and the LGM, when the forcings are changing relatively slowly and predominantly cool, destabilising the water column and favouring quicker adjustment. The Antarctic cold anomaly present at the end of the GHG and ALL experiments show that the warming ocean response during deglaciation is significantly distorted by the acceleration of the forcings, and for this reason our analysis of the ocean circulation concentrates on the earlier period.

The strength of both the AMOC and ACC both vary significantly in all of the simulations here. In our preindustrial run, the AMOC has a strength of 18.0 Sv, with deviations of up to 0.4 Sv on centennial timescales. In ALL-ZH, the AMOC maximum strength oscillates

between 15 and 20 Sv over the course of simulation, reaching its maximum strength at the LGM (Fig. 5). The AMOC strength in ALL-5G has a somewhat different response, showing an initial jump to a maximum strength of 23 Sv, which then slowly declines through the run until it reaches roughly the same strength as ALL-ZH at the LGM. In line with the smooth Greenland surface temperatures simulated by our experiments, neither of the ALL forcings experiments show any abrupt strengthening or weakening of the AMOC, likely due to the lack of meltwater runoff from the northern hemisphere ice-sheets in our experiments, although abrupt AMOC behaviour has been demonstrated in other experiments with FAMOUS (Smith and Gregory 2009; Hawkins et al. 2011).

There is some consensus that the AMOC at the LGM was shallower than today (Otto-Bliesner et al. 2007). Despite the similarities in the behaviour of the AMOC maxima in these two runs, the overall shape of the overturning structure in the Atlantic at the LGM does differ between the two ALL runs (Fig. 6). The AMOC in ALL-5G penetrates deeper than in ALL-ZH, with up to 4 Sv more NADW below 1,000 m in ALL-5G at the LGM.

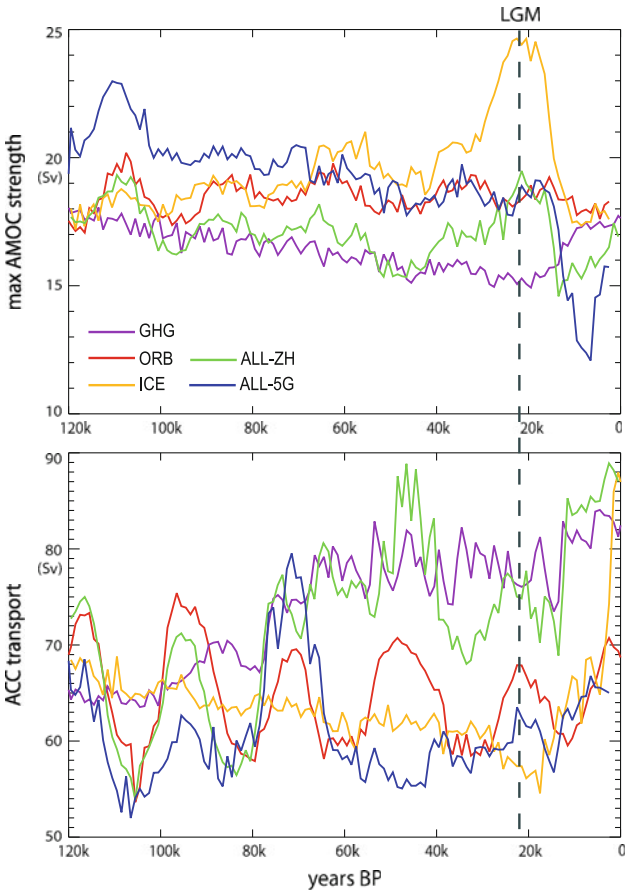

Fig. 5 Maximum AMOC (*top*) and ACC (*bottom*) strength through the simulations

AABW is consequently weaker in the LGM Atlantic in ALL-5G, with <2 Sv cell that extends no further north than 20°S, compared to the 3 Sv cell that reaches 20°N in ALL-ZH.

The ACC in the preindustrial run has a value of 67 ± 5 Sv, which is within the range of values simulated in the coupled model intercomparison database of Meehl et al. (2005). The ACC in ALL-ZH has initial ∼20 kyr oscillations of around ±10 Sv, before jumping up to a mean value of ∼75 Sv at 50 kyr BP (Fig. 5). The ACC in ALL-5G shows a substantially different response, with the initial ∼20 kyr oscillations being less regular in amplitude.

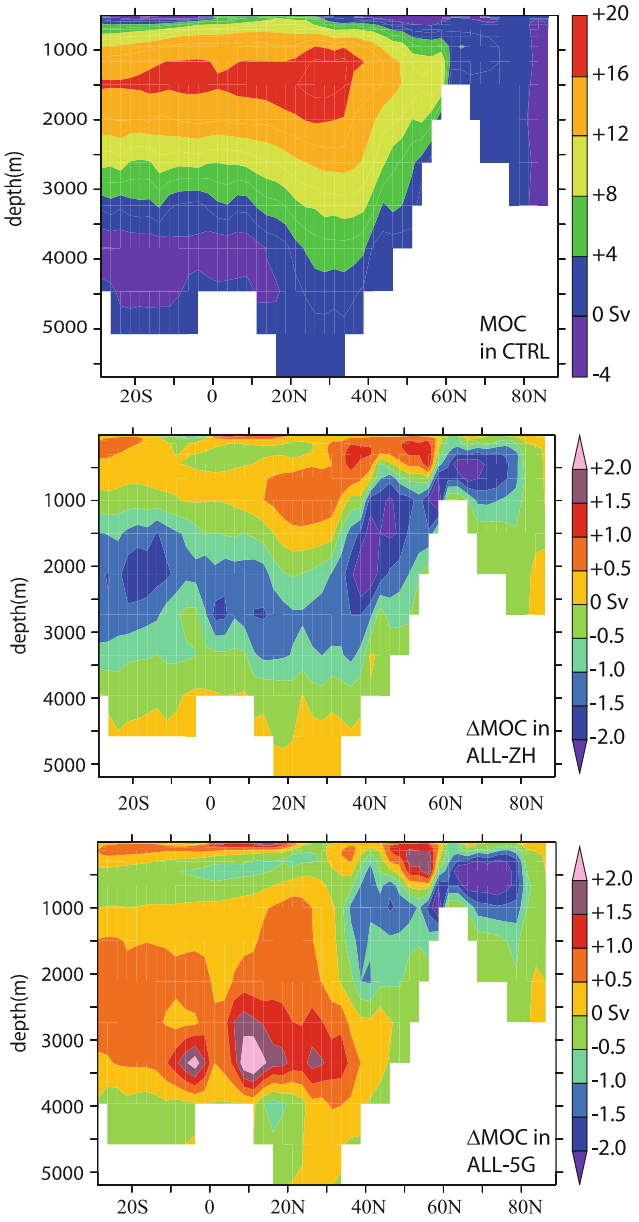

Fig. 6 AMOC streamfunction (positive indicates clockwise rotation) in the preindustrial (*top*), and differences at the LGM for ALL-ZH (*middle*) and ALL-5G (*bottom*)

The strength of the ACC is well correlated with the rate of AABW production (Gent et al. 2001), and similar variations also occur in the strength of the AABW cell simulated in the Atlantic. The difference between the ACC responses in the two ALL experiments shows a significant degree of sensitivity to the choice of northern hemisphere ice-sheet reconstruction. This is related to the stronger AMOC seen in ALL-5G, as cold deep water formed in the northern hemisphere flows south and significantly alters the barotropic meridional density gradient across the Southern Ocean, producing a weaker ACC. The sensitivity of the ACC to the AMOC does not carry through to Antarctic surface temperatures, however, which are similar in ALL-ZH and ALL-5G.

The changes in both the AMOC and the ACC in ALL-ZH are both reasonably well approximated by a linear addition of the responses seen in GHG, ICE and ORB. There is a degree of non-linear interaction which weakens the AMOC further as the climate cools. In GHG, the cooling effect of the glacial forcing acts to slow the AMOC by 3 Sv and increase the strength of the ACC by $\sim$10 Sv. In the North Atlantic there is an expansion of the sea-ice cover, which outweighs changes in the hydrological cycle and cooling of surface waters further south and acts as an insulating layer, reducing North Atlantic Deep Water (NADW) formation. In the southern hemisphere, the polar amplification effect that exaggerates high latitude temperature change increases the meridional temperature gradient over the Southern Ocean, which results in an increase in zonal wind stress and drives the ACC.

In ICE, the AMOC increases by 7 Sv as the ice-sheets grow, and the ACC slows by $\sim$10 Sv. The growing northern hemisphere ice-sheets cool the surface and result in colder and drier winds blowing across the Atlantic. This strongly cools the mid-latitude surface waters and allows for an increase in NADW formation. The ACC slows in ICE, despite there being no direct forcing in the southern hemisphere. This occurs as a result of the increase in NADW flowing into the South Atlantic and on to the Indian Ocean. This water reduces the barotropic meridional density gradient across the Southern Ocean, slowing the ACC. A similar relationship between the AMOC and ACC has been observed in other FAMOUS experiments, and this inter-hemispheric mechanism is also described in Fuckar and Vallis (2007).

In ORB, the both the AMOC and the ACC show a pronounced oscillation, with spectral analysis of the signal showing a strong peak with a period of around 20 kyrs. The amplitude of the AMOC oscillation is around 3 Sv in the early part of the simulation, but reduces to around 1 Sv by the end. The ACC oscillations have an initial amplitude of $\pm$10 Sv, reducing to $\pm$5 Sv by the end of the run. The AMOC and ACC variations are anti-correlated, with changes in the AMOC occurring $\sim$200 years earlier than those in the ACC. The character of these oscillations matches the precessional component of the orbital forcing, both in their period, and in the reduction in amplitude that occurs through the run as the effect of precession is modulated by the decreasing in eccentricity over the course of the run. Although the AMOC and ACC variations in ORB are anti-correlated, they appear to be at least partly independent. Further experiments, where variations in orbital forcing were restricted to certain latitude bands, show that oscillations of the same phase in the ACC can be forced by applying orbital forcing only at high southern latitudes, and in the AMOC be forcing by applying orbital forcing in the tropics. These seasonal orbital forcings are rectified by the ocean into changes in density gradients which force the respective circulations. Applying orbital forcing variations only at high northern latitudes does not produce significant changes in either the AMOC or the ACC.

There is some support for our simulated changes in the AMOC from analysis of ocean proxies as compilations of multi-proxy data point to significant variability in ocean circulation during the last glacial cycle (Rahmstorf 2002). Lisiecki et al. (2008) use multiple records of $\delta^{13}C$ to suggest that the AMOC responds significantly to precessional forcing with a minimum in overturning rates at June perihelion, but that the overall AMOC response is sensitive to factors other than summer insolation and ice volume. Although, in line with some previous studies (Yoshimori et al. 2001; Crucifix and Loutre 2005) we instead find maxima in AMOC strength corresponding to the June perihelion, the inclusion of the ice extent forcing in ALL-ZH does change the phase of the AMOC variability, particularly after $\sim$40 kyr BP. Rahmstorf (2002) concluded that there was evidence for three basic circulation regimes: a cold stadial state with reduced, shallower NADW and a shutdown state with no circulation, as well as a modern state with deep sinking in the North Atlantic. Although we do not see a shutdown state, the shallower LGM overturning in ALL-ZH corresponds to the suggested cold stadial state. More recently, Gherardi et al. (2009) use Pa/Th data from a number of cores to support the idea of a shallower, but slightly stronger AMOC at the LGM, and propose a range of other circulation patterns for different time periods, suggesting that a wider range of variability in the shape, not just the maximum strength, of the overturning streamfunction is likely to have occurred. Many ocean circulation proxy studies (including Gherardi et al. 2009) consider the evolution of the AMOC only since the LGM, however, and the evolution of the AMOC in our study is not robust in this most recent period due to the lack of abrupt events and the accelerated nature of our forcings. Care must then be taking in interpreting the detail of our results with the AMOC changes inferred from these proxies.

SV10 show the strength of the AMOC varying across a similar range of values to those seen in the ALL-5G run here, but there appears to be little correlation between their results and ours. They did not show any significant response of the AMOC to orbital forcing. This discrepancy may well be due to the snapshot nature of their experimental design. Their simulations for each period were started from a common preindustrial initial condition and run for 500 years. The deep ocean can take many hundreds of years to come into equilibrium with changed boundary conditions, so SV10's setup is unlikely to produce similar results to our accelerated transient experiments. This is especially true in the light of the discovery of AMOC bistability in FAMOUS (Hawkins et al. 2011), and the large differences we find between the ALL-ZH and ALL-5G runs; in both cases the transient history of the surface forcing plays a major role in setting the AMOC streamfunction.

7 Discussion and conclusion

We have presented results from a number of simulations of the last glacial cycle conducted with an AOGCM, which we believe are the first of their kind. An AOGCM suitable for multi-millennial simulations at relatively modest computational cost is a very useful tool for the simulation of transient climate change, and the favourable comparison of our results with climate reconstructions derived from proxy evidence bolsters confidence in the model.

A linear combination of the surface temperatures in the three individual forcing experiments (for instance, as shown in Fig. 1) is a good first-order approximation of the temperature evolution in experiment ALL-ZH. Given the complexity of the feedbacks in the climate system and the magnitude of the changes being forced here, this result is perhaps somewhat surprising. This linearity also extends to the simulated variability of the AMOC and ACC. This simplifies the task of dissecting the physical mechanisms at work in our simulations, if this linearity is realistic, is potentially helpful for understanding the real glacial climate system. However, despite our models's success in reproducing the long-term temperature changes from the ice-core temperature reconstructions, the lack of abrupt millennial-scale events from our simulations suggests that important feedbacks are missing from FAMOUS as used here, and this must cast doubt on whether the linearity of the climate forcings is, in fact, realistic.

The use of two different ice-sheet reconstructions in our experiments shows the sensitivity of the glacial climate system to ice-sheet forcing. Although LGM SSTs and Antarctic temperatures throughout the whole of the experiment seem little affected by the details of the northern hemisphere ice, experiments ALL-ZH and ALL-5G have developed significantly different northern hemisphere surface temperature patterns, AMOC structures and ACC strengths by the time of the LGM. The differences in AMOC strength through the two ALL simulations shows that the configuration of the ice over the whole of the glacial period is important for some aspects of the LGM as well as the climate in earlier periods. Features such as the AMOC that affect the density structure of the deep ocean are especially significant, as they impact ocean stratification and carbon storage that set glacial atmospheric CO_2. The differences in AMOC and AABW strength between ALL-ZH and ALL-5G lead to a deep ocean which is everywhere cooler (on average 0.5°C) in ALL-ZH by the LGM, and the differences in water temperature and deep ocean ventilation rates which produce this would be expected to have a significant effect on the draw-down of atmospheric CO_2. The over-estimate of the ICE-5G ice-sheet extent prior to the LGM in ALL-5G exaggerates the influence of ice-sheet forcing during the first part of the last glacial cycle in that simulation, so a more quantitative analysis is not justified here. The accelerated nature of the forcings used in these simulations is a further complication, as the distortion of the adjustment of the deep ocean to the surface forcings will also significantly affect the deep ocean structure.

Variations in the ocean circulation are some of the most interesting features of these runs, especially in light of their influence on deepwater formation and potential carbon storage in the ocean. Proxies for the large-scale circulation are few and far between, so it is difficult to validate the ocean variability seen in our experiments, but our results show that there is potential for large-scale changes in the ocean to play a role in regulating climate throughout the glacial cycle, not just during abrupt millennial events. Both the AMOC and the ACC respond strongly to the precessional component of the orbital forcing, despite the fact that it produces no annual average insolation change. The range of processes which we have shown affect the AMOC and ACC, and hence deepwater formation in the ocean, highlights the importance of conducting studies such as this with an AOGCM capable of reproducing a full range of processes that set the surface boundary conditions for the ocean.

An important aspect of the glacial climate system is the idea of the bipolar see-saw mechanism (Broecker et al. 1985), inferred from proxy data as affecting surface temperature during millennial scale climate events. Such a see-saw is not seen in our runs, either in terms of abrupt events, or anti-correlated surface temperature variations on any timescale. There is some evidence in our experiments, though, for the physical oceanic mechanism by which such a see-saw might work, in the anti-correlated interplay between the AMOC and the ACC. Support for an AMOC-

mediated Greenland/Antarctic temperature see-saw is often claimed to have been provided by modelling studies, although this is perhaps overstated, with only models of intermediate complexity with simplified atmospheres showing a significant surface temperature change on Antarctica itself (e.g. Ganopolski and Rahmstorf 2001). Other studies using coupled AOGCMs have found differing results, which they attribute to internal variability, or different mechanisms (e.g. Rind et al. 2001; Vellinga and Wood 2002). Wolff et al.'s (2009) recent hypothesis linking southern and northern hemisphere climate events requires a physical ocean teleconnection, and one in which the coupling breaks down at the LGM, initiating deglaciation. In our runs, the degree of the coupling between the two hemispheres does change through the glacial, with the coupling reducing in strength as the northern hemisphere ice-sheets build and provide a strong local influence on the AMOC, and the ocean fills with cold glacial deepwater. Wolff et al. (2009) require the see-saw to be led by the southern hemisphere, which is not seen clearly in our experiments. We did, however, simulate variations in the AMOC which were well correlated with variations in the transport of Indian Ocean water to the Atlantic. In FAMOUS, this transport can be altered by changes in the path of the ACC as it flows past Africa. A southern hemisphere forcing (for example, a shift in the southern hemisphere westerlies) which caused a shift in the path of the ACC could then account for the inter-hemispheric link with a southern lead.

The use of an AOGCM allows an unprecedented resolution of the surface climate over land through the glacial cycle. Our results show, perhaps unsurprisingly, that surface temperature changes through the experiments are not zonally uniform, especially in the northern hemisphere, and care should thus be taken in interpreting Greenland ice-core data as being representative of high northern latitudes as a whole. Analysis of the simulation of the atmospheric circulation through the glacial cycle will be the focus of future work.

There are a number of important simplifications used in this study whose potential influences should not be forgotten. Perhaps chief amongst these is the acceleration of the forcing factors, which distorts the response of slow processes in the deep ocean. Although this does not appear to be the cause of the anomalously slow surface cooling we find during glacial inception, it is almost certainly to blame for the slow rate of warming in the southern hemisphere during deglaciation, and probably adversely affects the model's simulated AMOC response. Given the lag that is present in our deep-ocean response to deglaciation, our results, especially for this part of the simulation, should be interpreted with caution. Issues such as this, and the approximations inherent in any climate model (which are particularly pronounced in models computationally cheap enough to simulate several millennia within a practical time-frame) mean that an experiment such as ours focuses attention on the abilities and limitations of the modelling approach itself. A detailed evaluation of paleoclimate simulations is often prevented by a lack of suitable observations, but can be facilitated by comparisons with simulations from models that occupy other positions in the hierarchy of complexity. In future work with FAMOUS and other models, we will further pursue such evaluation.

Alternative approaches could be taken to the simplifications we made in order to better simulate different aspects of the glacial climate. Specific periods of interest—deglaciation, for instance—could be run separately without the acceleration, relying on the assumption that the initial state produced through the accelerated run was appropriate. Alternatively, accelerated timestepping schemes (e.g. Bryan 1984) could be used to try to speed up the deep ocean adjustment, although this would distort the ocean response in other ways, or asynchronous coupling employed (Voss et al. 1998) at the expense of the accuracy of the atmosphere–ocean feedbacks. However, given the computational expense of atmospheric GCMs, it is currently not possible to do without some kind of timestepping shortcut if we wish to retain the level of detail and complexity provided by the atmosphere in this study. Although similar studies have been conducted with less complex models (e.g. Holden et al. 2010; Ganopolski et al. 2010), which have obtained results that compare well with the gross features of proxy-based climate reconstructions, the greater complexity of AOGCMs allow the some of the behaviour and feedbacks at play in the glacial climate to be studied in a setting that is less prescribed than in a less complex model.

Of the three independent forcing factors used in this study, only the orbital forcing is actually external to the real climate. Both GHGs and ice-sheets have important feedbacks with the rest of the climate system, and a full understanding of glacial cycles cannot be gained without modelling these features interactively. The processes by which sufficient quantities of carbon are drawn down into the glacial ocean to produce the atmospheric CO_2 concentrations seen in ice-core records are not well understood, and have to date not been successfully modelled by a realistic coupled model. FAMOUS, as used in this study, does have a simple marine biogeochemistry model, although it does not respond to the forcings in these simulations in a way that would imply an increased uptake of carbon. A further FAMOUS simulation with interactive atmospheric CO_2 did not produce any significant changes in atmospheric CO_2 during the early glacial when forced with orbital variations and a growing northern hemisphere ice-sheet. Accurately modelling a glacial cycle with

interactive carbon chemistry requires a significant increase in our understanding of the processes involved, not simply the inclusion of a little extra complexity to the current model.

The non-interactive nature of the ice-sheets here touches on another grand challenge of Earth system modelling. Coupling ice-sheet and atmosphere models at the high resolutions required to model the feedbacks accurately over timescales required for the evolution of the ice-sheet is currently impractical, and as such cannot be included in a study such as this. Interactive ice-sheets are not only required for correctly simulating the large-scale, long-term evolution of climate through glacial cycles but also abrupt climate events, as runoff or meltwater feed into the ocean and disrupt the ocean circulation. Future development work with FAMOUS will concentrate on new subgrid-scale parameterisations to attempt to efficiently include ice-sheet-atmosphere feedbacks.

These simulations have produced $\sim$1 TB of decadal and monthly mean data. Any one paper such as this can only address a limited number of features of the simulations, and further studies on different aspects of the climate system will be forthcoming. In addition the data will also be archived at the British Atmospheric Data Centre (http://www.badc.ac.uk) where it will be accessible to the community.

Acknowledgments This paper was improved following discussions with our anonymous reviewer, whom we would like to thank. We would like to acknowledge the support of Simon Wilson and other members of the NCAS Computer Modelling Support Team in this work. The work was supported by grants from the UK RAPID (NER/T/S/2002/00462), Quaternary QUEST (NE/D00182X/1) and QUEST-ESM projects. Jonathan Gregory was partly supported by the Joint DECC, Defra and MoD Integrated Climate Programme, GA01101 (DECC/Defra). We thank Valerie Masson-Delmotte for providing us with NGRIP temperature reconstruction data, and Philippe Huybrechts for providing his ice-sheet reconstruction.

References

Archer D, Winguth A, Lea D, Mahowald N (2000) What caused the glacial/interglacial atmospheric pCO_2 cycles. Rev Geophys 38(2):159–189

Berger AL (1978) Long-term variations of daily insolation and quaternary climatic change. J Atmos Sci 35:2362–2367

Blunier T, Chappellaz J, Schwander J, Dallenbach A, Stauffer B, Stocker TF, Raynaud D, Jouzel J, Clausen HB, Hammer CU, Johnsen SJ (1998) Asynchrony of Antarctic and Greenland climate change during the last glacial period. Nature 394: 739–743

Bond G, Broecker W, Johnsen S, McManus J, Labeyrie L, Jouzel J, Bonani G (1993) Correlations between climate records from North Atlantic sediments and Greenland ice. Nature 365:143–147

Braconnot P, Otto-Bliesner B, Harrison S, Joussaume S, Peterchmitt J-Y, Abe-Ouchi A, Crucifix M, Driesschaert E, Fichefet T, Hewitt CD, Kageyama M, Kitoh A, Laîné A, Loutre M-F, Marti O, Merkel U, Ramstein G, Valdes P, Weber SL, Yu Y, Zhao Y (2007) Results of PMIP2 coupled simulations of the mid-Holocene and Last Glacial Maximum—Part 1: experiments and large-scale features. Clim Past 3:261–277

Broecker W, Peteet DM, Rind D (1985) Does the ocean–atmosphere system have more than one stable mode of operation? Nature 315:21–26

Bryan K (1984) Accelerating the convergence to equilibrium of ocean-climate models. J Phys Oceanogr 14:666–673

Clark PU, Alley RB, Pollard D (1999) Northern hemisphere ice-sheet influences on global climate change. Science 286:1104–1110

Crucifix M, Loutre MF (2005) Transient simulations over the last interglacial period (125–115 kyr bp): feedback and forcing analysis. Clim Dyn 24:279–295

EPICA Community Members (2006) One-to-one coupling of glacial climate variability in Greenland and Antarctica. Nature 444:195–198

Fuckar NS, Vallis GK (2007) Interhemispheric influence of surface buoyancy conditions on a circumpolar current. Geophys Res Lett 34. doi:10.1029/2007GL030379

Ganopolski A, Rahmstorf S (2001) Rapid changes of glacial climate simulated in a coupled climate model. Nature 409:153–158

Ganopolski A, Calov R, Claussen M (2010) Simulation of the last glacial cycle with a coupled climate ice-sheet model of intermediate complexity. Clim Past 6:229–244

Gent PR, Large WG, Bryan FO (2001) What sets the mean transport through the Drake Passage? J Geophys Res 106:2693–2712

Gherardi J-M, Labeyrie L, Nave S, Francois R, McManus JF, Cortijo E (2009) Glacial-interglacial circulation changes inferred from $^{231}Pa/^{230}Th$ sedimentary record in the North Atlantic region. Paleoceanography 24:PA2204. doi:10.1029/2008PA001696

Gordon C, Cooper C, Senior CA, Banks H, Gregory JM, Johns TC, Mitchell JFB, Wood RA (2000) The simulation of SST, sea ice extents and ocean heat transports in a version of the Hadley Centre coupled model without flux adjustments. Clim Dyn 16:147–168

Gregory JM, Huybrechts P (2006) Ice-sheet contributions to future sea-level change. Philos Trans R Soc Lond 364:1709–1731. doi:10.1098/rsta.2006.1796

Hawkins E, Smith RS, Allison LC, Gregory JM, Woollings TJ, Pohlmann H, de Cuevas B (2011) Bistability of the Atlantic overturning circulation in a global climate model and links to ocean freshwater transport. Geophys Res Lett 38. doi:10.1029/2011GL047208

Hays JD, Imbrie J, Shackelton NJ (1976) Variations in the earth's orbit: pacemaker of the ice ages. Science 194:1121–1132

Hewitt CD, Mitchell JFB (1997) Radiative forcing and response of a GCM to ice age boundary conditions: cloud feedback and climate sensitivity. Clim Dyn 13:821–834

Hewitt CD, Stouffer RJ, Broccoli AJ, Mitchell JFB, Valdes PJ (2003) The effect of ocean dynamics in a coupled GCM simulation of the Last Glacial Maximum. Clim Dyn 20:203–218. doi:10.1007/s00382-002-0272-6

Holden PB, Edwards NR, Wolff EW, Lang NJ, Singarayer JS, Valdes PJ, Stocker TF (2010) Interhemispheric coupling and warm Antarctic interglacials. Clim Past 6:431–443

Huybers P, Wunsch C (2005) Obliquity pacing of the late Pleistocene glacial terminations. Nature 434:491–494

Jones C (2003) A fast ocean GCM without flux adjustments. J Atmos Ocean Technol 20:1857–1868

Jones C, Gregory J, Thorpe R, Cox P, Murphy J, Sexton D, Valdes P (2005) Systematic optimisation and climate simulations of FAMOUS, a fast version of HadCM3. Clim Dyn 25:189–204

Jouzel J, Masson-Delmotte V, Cattani O, Dreyfus G, Falourd S, Hoffmann G, Minster B, Nouet J, Barnola JM, Chappellaz J, Fischer H, Gallet JC, Johnsen S, Leuenberger M, Loulergue L, Luethi D, Oerter H, Parrenin F, Raisbeck G, Raynaud D, Schilt A, Schwander J, Selmo E, Souchez R, Spahni R, Stauffer B, Steffensen JP, Stenni B, Stocker TF, Tison JL, Werner M, Wolff EW (2007) Orbital and millennial Antarctic climate variability over the past 800,000 years. Science 317:793–797

Justino F, Timmermann A, Merkel U, Peltier WR (2006) An initial intercomparison of atmospheric and oceanic climatology for the ICE-5G and ICE-4G models of LGM paleotopography. J Clim 19:3–14

Lisiecki LE, Raymo ME (2005) A Pliocene–Pleistocene stack of 57 globally distributed benthic $\delta^{18}O$ records. Paleoceanography 20. doi:10.1029/2004PA001071.

Lisiecki LE, Raymo ME, Curry WB (2008) Atlantic overturning responses to late Pleistocene climate forcings. Nature 456:85–88

Lunt DJ, Foster GL, Haywood AM, Stone EJ (2008) Late Pliocene Greenland glaciation controlled by a decline in atmospheric CO_2 levels. Nature 454:1102–1105

Lüthi D, Le Floch M, Bereiter B, Blunier T, Barnola J-M, Siegenthaler U, Raynaud D, Jouzel J, Fischer H, Kawamura K, Stocker TF (2008) High-resolution carbon dioxide concentration record 650,000–800,000 years before present. Nature 453: 379–382

Manabe S, Wetherald R (1975) The effects of doubling the CO_2 concentration on the climate of a general circulation model. J Atmos Sci 32:3–15

MARGO Project Members (2009) Constraints on the magnitude and patterns of ocean cooling at the Last Glacial Maximum. Nature Geosci 2:127–132

Marsh R, Smith MPLM, Rohling EJ, Lunt DJ, Lenton TM, Williamson MS, Yool A (2006) Modelling ocean circulation, climate and oxygen isotopes in the ocean over the last 120,000 years. Clim Past Discuss 2:657–709

Martinson DG, Pisias NG, Hays JD, Imbrie J, Moore TC, Shackleton NJ (1987) Age dating and the orbital theory of the ice ages—development of a high-resolution 0 to 300,000-year chronostratigraphy. Quat Res 27:1–29

Masson-Delmotte V, Jouzel J, Landais A, Stievenard M, Johnsen SJ, White JWC, Werner M, Sveinbjornsdottir A, Fuhrer K (2005) GRIP deuterium excess reveals rapid and orbital-scale changes in Greenland moisture origin. Science 309:118–121

Masson-Delmotte V, Stenni B, Pol K, Braconnot P, Cattani O, Falourd S, Kageyama M, Jouzel J, Landais A, Minster B, Barnola JM, Chappellaz J, Krinner G, Johnsen S, Röthlisberger R, Hansen J, Mikolajewicz U, Otto-Bliesner B (2010) EPICA Dome C record of glacial and interglacial intensities. Quat Sci Rev 29:113–128

Meehl GA, Covey C, McAvaney B, Latif M, Stouffer RJ (2005) Overview of the Coupled Model Intercomparison Project. Bull Am Meteorol Soc 86(1):89–93

Otto-Bliesner B, Hewitt CD, Marchitto TM, Brady E, Abe-Ouchi A, Crucifix M, Murakami S, Weber SL (2007) Last Glacial Maximum ocean thermohaline circulation: PMIP2 model intercomparisons and data constraints. Geophys Res Lett 340. doi: 10.1029/2007GL029475

Otto-Bliesner BL, Schneider R, Brady EC, Kucera M, Abe-Ouchi A, Bard E, Braconnot P, Crucifix M, Hewitt CD, Kageyama M, Marti O, Paul A, Rosell-Melé A, Waelbroeck C, Weber SL, Weinelt M, Yu Y (2009) A comparison of PMIP2 model simulations and the MARGO proxy reconstruction for tropical sea surface temperatures at Last Glacial Maximum. Clim Dyn 32:799–815

Pacanowski RC, Dixon K, Rosati A (1990) The GFDL modular ocean model users guide: version 1.0. technical report 2. Geophysical Fluid Dynamics Laboratory/NOAA, Princeton University

Parrenin F, Barnola J-M, Beer J, Blunier T, Castellano E, Chappellaz JA, Dreyfus G, Fischer H, Fujita S, Jouzel J, Kawamura K, Lemieux-Dudon B, Loulergue L, Masson-Delmotte V, Narcisi B, Petit J-R, Raisbeck G, Raynaud D, Ruth U, Schwander J, Severi M, Spahni R, Steffensen JP, Svensson AM, Udisti R, Waelbroeck C, Wolff EW (2007) The EDC3 chronology for the EPICA Dome C ice core. Clim Past 3:485–497

Peltier WR (2004) Global glacial isostasy and the surface of the ice-age earth: the ICE-5G (VM2) model and GRACE. Ann Rev Earth Planet Sci 32:111–149

Rahmstorf S (2002) Ocean circulation and climate during the past 120,000 years. Nature 419:207–214

Rind D, Russell GL, Schmidt GA, Sheth S, Collins D, Demenocal P, Teller J (2001) Effects of glacial meltwater in the GISS coupled atmosphere–ocean model: Part II: a bi-polar seesaw in Atlantic deep water production. J Geophys Res 106:27355–27366

Singarayer JS, Valdes PJ (2010) High-latitude climate sensitivity to ice-sheet forcing over the last 120 kyr. Quat Sci Rev 29:43–55

Smith RS, Gregory JM (2009) A sensitivity study on the impact of freshwater input in different regions of the North Atlantic. Geophys Res Lett 36. doi:10.1029/2009GL038607

Smith RS, Osprey A, Gregory JM (2008) A description of the FAMOUS (version XDBUA) climate model and control run. Geosci Model Dev 1:53–68

Spahni R, Chappellaz J, Stocker TF, Loulergue L, Hausammann G, Kawamura K, Flückiger J, Schwander J, Raynaud D, Masson-Delmotte V, Jouzel J (2005) Atmospheric methane and nitrous oxide of the late Pleistocene from Antarctic ice cores. Science 310:1317–1321. doi:10.1126/science.1120132

Thomas ER, Wolff EW, Mulvaney R, Steffensen JP, Johnsen SJ, Arrowsmith C (2009) Anatomy of a Dansgaard-Oeschger warming transition—high resolution analysis of the NGRIP ice core. J Geophys Res 114. doi:10.1029/2008JD011215

Timm O, Timmermann A (2007) Simulation of the last 21,000 years using accelerated transient boundary conditions. J Clim 20:4377–4401

Tindall JC, Valdes PJ, Sime LC (2009) Stable water isotopes in HadCM3 the isotopic signature of ENSO and the tropical amount effect. J Geophys Res 114. doi:10.1029/2008JD010825

Vellinga M, Wood RA (2002) Global climatic impacts of a collapse of the Atlantic thermohaline circulation. Clim Change 54(3):251–267

Voss R, Sausen R, Cubasch U (1998) Periodically synchronously coupled integrations with the atmosphere–ocean general circulation model ECHAM3/LSG. Clim Dyn 14:249–266

Wolff EW, Fischer H, Rothlisberger R (2009) Glacial terminations as southern warmings without northern control. Nat Geosci 2:206–209

Wolff EW, Chappellaz J, Blunier T, Rasmussen SO, Svensson A (2010) Millennial-scale variability during the last glacial: the ice core record. Quat Sci Rev 29. doi:10.1016/j.quascirev.2009.10.013

Wunsch C (2006) Abrupt climate change. An alternative view. Quat Res 65:191–203

Yoshimori M, Weaver AJ, Marshall SJ, Clarke GKC (2001) Glacial termination: sensitivity to orbital and CO_2 forcing in a coupled climate system model. Clim Dyn 17:571–588

Zweck C, Huybrechts P (2005) Modeling of the northern hemisphere ice sheets during the last glacial cycle and glaciological sensitivity. J Geophys Res 110:D07103. doi:10.1029/2004JD005489